Available online at www.sciencedirect.com

ScienceDirect

Scripta Materialia 90–91 (2014) 45–48

Scripta MATERIALIA

www.elsevier.com/locate/scriptamat

Room-temperature creep resistance of Co-based metallic glasses

P.F. Yu,[a] S.D. Feng,[a] G.S. Xu,[a] X.L. Guo,[a] Y.Y. Wang,[a] W. Zhao,[a] L. Qi,[a] G. Li,[a,b,*] P.K. Liaw[b] and R.P. Liu[a]

[a] *State Key Laboratory of Metastable Materials Science and Technology, Yanshan University, Qinhuangdao 066004, China*
[b] *Department of Materials Science and Engineering, The University of Tennessee, Knoxville, TN 37996-2200, USA*

Received 28 June 2014; accepted 25 July 2014
Available online 1 August 2014

The room-temperature creep resistance of the $Co_{56}Ta_9B_{35}$ metallic glass was determined by a nanoindentation technique. Results showed that the creep curves were described by a generalized Kelvin model. The low creep strain-rate sensitivity parameter and creep rate derived from the displacement–holding time curves demonstrated the high creep resistance of the $Co_{56}Ta_9B_{35}$ metallic glass. The deformation mechanism causing the nanoindentation creep was discussed based on the "shear transformation zone" concept, which gave an explanation for the creep behavior in metallic glasses.

Keywords: Metallic glasses; Nanoindentation; Creep resistance; Shear transformation zone

A number of Co-based multicomponent metallic glass (MG) systems have been reported, including Co–Fe–(Ta,Mo)–(B,Si) [1–4], (Co–Fe)–(Nb,Zr)–(B,Si) [5–9], (Co,Fe,Ni)–(Zr,Hf,Nb,Ta,Mo,W)–B [10] and Co–Fe–B–Si [11]. The family of Co-based MGs has been widely studied in recent decades. A wide range of material properties have been investigated, including glass-forming ability [7–9], thermal stability, strength [1–3,8] and magnetic properties [2,7,9–11]. For instance, the $Co_{43}Fe_{20}Ta_{5.5}B_{31.5}$ MG has been reported to be the strongest MG [2] with promising magnetic applications [1,2,4,12–14]. The tensile strengths of Co–Si–B and Co–Ta–Si–B alloys have been reported to range from 3580 to 4000 MPa, respectively. When Fe is removed from the Co–Fe–Ta–B ribbon and wire MGs [12], the fracture strength of Co-based MGs can even increase to above 6000 MPa.

$Co_{65-x}Ta_xB_{35}$ (at.%, $x = 5$–11) [12,15] systems have rapidly become of broad interest, having set the record for the highest strength among the known bulk glassy alloys, with an elastic modulus and hardness of 280 and 17.8 GPa, respectively. Our recent research [15,16] on the compressibility of CoTaB MGs under high pressure by using synchrotron radiation X-ray diffraction (XRD) confirmed that the charge density and bonding character demonstrate that the covalent character of Co–B and B–B bonds is the reason for the high elastic modulus and hardness in CoTaB MGs [15].

Very recently, a plasticity ternary $Co_{61}Nb_8B_{31}$ bulk MG was fabricated with a plasticity of 5% and a yield strength of 5200 MPa [17]. However, the room-temperature creep-resistance behavior of Co-based MGs has not been reported. The plastic deformation of MGs and the related mechanism are considered to be among the most important aspects of their engineering application. Thus, studying the creep-resistance behavior of materials can enable the selection of appropriate materials in different environments. Given the size limitation of MGs, many of their mechanical properties cannot be studied by traditional methods. A new nanoindentation technique has recently paved a new path for research on the plastic deformation of glassy alloys [18]. Therefore, in this work, we use $Co_{56}Ta_9B_{35}$ as a model MG to study the creep-resistance behavior at room temperature using the nanoindentation technique.

The amorphous ribbon was prepared by the melt-spinning technique in an argon atmosphere. The glassy structure of the alloys was ascertained by XRD using a D/MAX-2500/PC diffractometer with Cu K_α radiation

* Corresponding author at: State Key Laboratory of Metastable Materials Science and Technology, Yanshan University, Qinhuangdao 066004, China. Tel./fax: +86 335 8074545; e-mail addresses: gli25@utk.edu; gongli@ysu.edu.cn

http://dx.doi.org/10.1016/j.scriptamat.2014.07.013
1359-6462/

($\lambda = 1.54$ Å). The thermal stability of ribbons was determined using a NETZSCH STA449C differential scanning calorimetry (DSC) device at a heating rate of 20 K min^{-1}. Nanoindentation experiments were conducted on a nanoindenter Hysitron TriboIndenter with a diamond Berkovich tip having a 260 nm radius of curvature. Hardness and Young's modulus were investigated according to the analysis of Oliver and Pharr [19]. Creep measurements were performed as follows. The load was increased up to the maximum load, P_{max}, of 4000 μN at different loading rates, dP/dt, of 40, 100 and 400 μN s^{-1}. The indenter was held at P_{max} for 60 s to measure the time-dependent displacement, and the unloading kept the same rate as the loading rate. The indenter was then unloaded to 10% of the maximum load and held for the thermal drift correction. The data were averaged in groups of five.

Figure 1(a) shows the XRD pattern of the amorphous ribbon. The broad diffraction maxima and absence of Bragg peaks corresponding to the crystalline phase in the XRD curves are characteristic of an amorphous structure.

Based on the DSC trace in Figure 1(b), the glass-transition temperature (T_g), crystallization temperature (T_x), crystallization peak temperature (T_p) and supercooled liquid region, ΔT_x, ($\Delta T_x = T_x - T_g$) were determined to be 964.5, 1,014, 1,023 and 49.5 K, respectively. The $Co_{56}Ta_9B_{35}$ MGs exhibited both a high glass-transition temperature and a large super-cooled liquid region, which are highly favorable for the extensive application of MGs as structural materials because of their high thermal stability.

Figure 2 presents load–displacement (P–h) nanoindentation curves obtained under a load control mode for loading rates of 40, 100 and 400 μN s^{-1}. The apparent absence of serrations at small depths (<60 nm) may be the reason for either the lack of resolution of the system or the fully elastic response of the material in the first few nanometers of penetration. Pop-in events appear clearly in the low loading curves, but they become imperceptible at the high loading rate. The creep platforms appear at different loading rates, while larger displacements are observed for higher loading rates (3 nm for 400 μN s^{-1}), suggesting that, for high rates, the plastic flow, which was not produced during the loading stage, occurs during the force-holding stage.

Figure 3 shows the experimental data of $Co_{56}Ta_9B_{35}$ MG with the creep at 4000 μN. The indenter displacement rapidly increased at the beginning of the holding

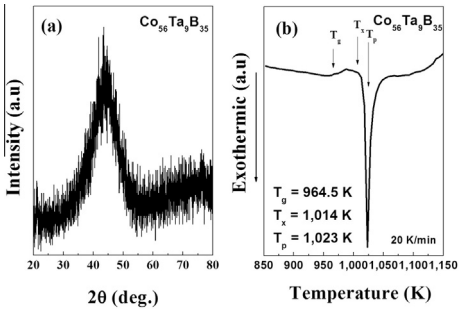

Figure 1. XRD pattern (a) and DSC trace (b) of the $Co_{56}Ta_9B_{35}$ MG, showing the T_g, T_x and T_p.

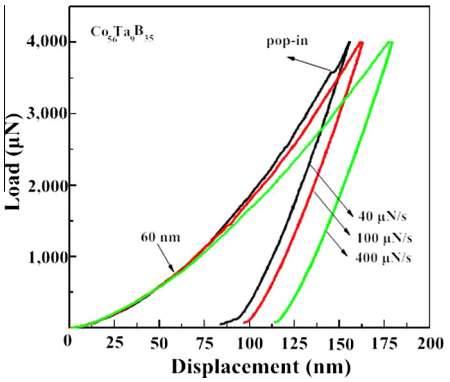

Figure 2. P–h curves measured during nanoindentation tests in a load control mode at loading rates of 40, 100 and 400 μN s^{-1}.

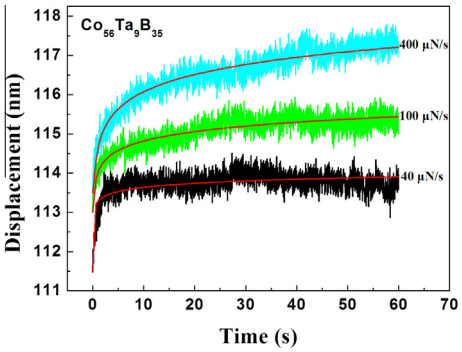

Figure 3. Creep displacement vs. time of the $Co_{56}Ta_9B_{35}$ MG at different loading rates. Red solid lines are curve-fitting results. (For interpretation of the references to colour in this figure legend, the reader is referred to the web version of this article.)

period and then approached a steady state at the end of the creep curve. The results showed that a faster strain rate resulted in the larger creep displacement. The creep displacement (h) and creep rate ($\varepsilon_s = \frac{dh}{dt}$) of $Co_{56}Ta_9B_{35}$ can be obtained from Figure 3 and are summarized in Table 1.

Viscoelastic (anelastic and viscoplastic) deformation can generally be described as a series of linear springs and dashpots, known as the Kelvin model. This model is commonly used to describe the creep of polymers [20–22], but can also be used for MGs (e.g. [23]), i.e.

$$h = \sum_{i=1}^{n} h_i\left(1 - e^{-\frac{t}{\tau_i}}\right) + \frac{t}{\mu_0} \quad (1)$$

where h_i is the indentation depth and τ_i is the characteristic relaxation time for the activation of the ith anelastic process. In the second term on the right-hand side of Eq. (1), t is the experimental time and μ_0 is a constant proportional to the viscosity coefficient of the last dashpot.

The creep curves in Figure 3 are successfully fitted by a series of two exponential decays representing the anelastic deformation plus the viscoplastic contribution, t/μ_0. Notably, Figure 3 shows this for a typical displacement–holding time curve. Eq. (1) can simulate the experimentally measured creep rate of the present MG with high accuracy (correlation coefficient $R^2 > 0.98$ for all tests).